Inorg. Chem. **2004**, *43*, 5283–5293

Synthesis and Characterization of a New Bisphosphonic Acid and Several Metal Hybrids Derivatives

M. Mar Gómez-Alcántara,[†] Aurelio Cabeza,[†] María Martínez-Lara,[†] Miguel A. G. Aranda,*[,†] Rafael Suau,[‡] Nattamai Bhuvanesh,[§] and Abraham Clearfield[§]

Departamento de Química Inorgánica and Departamento de Química Orgánica, Universidad de Málaga, Campus Teatinos, 29071 Málaga, Spain, and Department of Chemistry, Texas A & M University, College Station, Texas 77842-3012

Received April 28, 2004

Commercial bis-(4-bromophenyl)-ether, $[BrC_6H_4]_2$–O, has been used to prepare 4-[4′-(diethoxyphosphoryl)phenoxy]phenyl-phosphonic acid diethyl ester, $[(CH_3CH_2)_2O_3P–C_6H_4]_2$–O, (**I**) following a slight modification of the Michaelis–Arbuzov reaction. The acid hydrolysis of **I** gave 4-(4′-phosphonophenoxy)phenyl phosphonic acid, $[H_2O_3P–C_6H_4]_2$–O (**II**), and both compounds have been characterized by ^{1}H NMR and ^{13}C NMR. The crystal structure of **II** has been determined by single-crystal X-ray diffraction. **II** crystallizes in an orthorhombic unit cell, space group *Pbcn*, with $a = 7.822(3)$ Å, $b = 5.821(2)$ Å, $c = 28.982(9)$ Å, and $V = 1319.7(7)$ Å^3. The final R factor was R1 = 0.0614. The structure is layered, being held together through a hydrogen bonding network. **II** has been used as precursor in the syntheses of new metal (Mn, Fe, Co, Ni, Cu, and Zn) bisphosphonates. The syntheses were carried out using a fixed metal/bisphosphonic acid molar ratio of 2.1:1 and the influence of the pH in the reactions has been studied. Nine new compounds have been isolated: $Mn_2(O_3PC_6H_4OC_6H_4PO_3)\cdot 1.5H_2O$ (**III**), $Mn_5(OH)_2(O_3PC_6H_4OC_6H_4PO_3)_2\cdot 2H_2O$ (**IV**), $Fe(HO_3PC_6H_4OC_6H_4PO_3)\cdot 0.5H_2O$ (**V**), $Co_2(O_3PC_6H_4OC_6H_4PO_3)\cdot 2H_2O$ (**VI**), $Ni_2(O_3PC_6H_4OC_6H_4PO_3)\cdot 3H_2O$ (**VII**), $Ni_2(O_3PC_6H_4OC_6H_4PO_3)\cdot 2H_2O$ (**VIII**), $Cu_2(O_3PC_6H_4OC_6H_4PO_3)$ (**IX**), $Zn_2(O_3PC_6H_4OC_6H_4PO_3)$ (**X**), and $Zn(HO_3PC_6H_4OC_6H_4PO_3H)$ (**XI**). Compound **IX** crystallizes in an orthorhombic unit cell, space group *Pbcn*, and unit cell parameters $a = 8.1012(5)$ Å, $b = 5.3109(3)$ Å, $c = 29.2595(5)$ Å, and $V = 1258.8(1)$ Å^3. Its structure has been solved by ab initio powder diffraction and refined by the Rietveld method to $R_F = 0.042$. **IX** has a pillared layer framework with highly distorted CuO_5 groups sharing edges to give isolated dimers. **XI** was indexed in a monoclinic unit cell, space group $P112_1$, with parameters $a = 9.4991(9)$ Å, $b = 5.0445(5)$ Å, $c = 29.131(2)$ Å, $\gamma = 91.945(7)°$, and $V = 1395.1(3)$ Å^3. Its structure has been refined by the Rietveld method, $R_F = 0.054$, since it is isostructural with the known compound, $Zn[HO_3P(C_6H_4)_2PO_3H]$. All solids were also characterized by thermal analysis and IR and UV–Vis spectroscopies.

Introduction

Hybrid organo−inorganic solids provide numerous compounds whose frameworks are built from the ionocovalent connection of inorganic moieties via organic molecules functionalized by complexing groups such as carboxylates or phosphonates, with the dimensionality of the final solid being largely influenced by the number of complexing groups.[1−4] During the past few decades, much effort has been dedicated to obtaining porous materials by using organodiphosphonate ligands ($[O_3P−R−PO_3]^{4−}$, R = organic unit) whose combinations with metals are expected to lead to three-dimensional structures with open frameworks without using any organic template. Moreover, the use of alkyl and/or aryl diphosphonates could allow manipulation of the length of the carbon chains to increment and modulate the size of the pores. In general, microporous materials are of great im-

* Author to whom correspondence should be addressed. E-mail: g_aranda@uma.es.
[†] Departamento de Química Inorgánica, Universidad de Málaga.
[‡] Departamento de Química Orgánica, Universidad de Málaga.
[§] Texas A & M University.

(1) Barthelet, K.; Nogues, M.; Riou, D.; Férey, G. *Chem. Mater.* **2002**, *14*, 4910−4918.
(2) (a) Clearfield, A. *Progress in Inorganic Chemistry*; Karlin, K. D., Ed.; John Wiley & Sons: New York, 1998; vol. 47, pp 371−510. (b) Clearfield, A. *Curr. Opin. Solid State Mater. Sci.* **2002**, *6*, 495−506.
(3) Eddaoudi, M.; Kim, J.; Rosi, N.; Vodak, D.; Wachter, J.; O'Keeffe, M.; Yaghi, O. *Science* **2002**, *295*, 469.
(4) Forster, P. M.; Cheetham, A. K. *Top. Catal.* **2003**, *1−4*, 79−86.

10.1021/ic049453l CCC: $27.50
Published on Web 07/17/2004

portance as molecular sieves, catalysts, ion-exchangers, and sensor materials.[2a,5]

Two main strategies have been followed to synthesize a vast number of new compounds of di-, tri-, and tetravalent metals: (1) using alkylenediphosphonic acids [$-O_3P(CH_2)_nPO_3-$, mainly for $n = 1-5$ and 8], and (2) using arylbisphosphonic acids; with or without introducing in the syntheses a second organic ligand or spacers such as phosphites or phosphates.[2a,3f,6] The organic phosphonate units act as cross-linking agents which covalently pillar the metal inorganic layers giving the hybrid materials. In general, whatever the nature of the cation and the length of the chain, the porosity of the final compounds is crucially related to the rigidity of the organic linker.[6c] Methylendiphosphonates provide the more open structures in the group of alkyldiphosphonates. So, $NaZn_2(OH)(O_3P-CH_2-PO_3)\cdot 1.5H_2O$ shows a zeotype structure with 10-membered channels built up from the corner-sharing of two types of monodimensional moieties: infinite chains of tetrahedral and columns of hexameric units containing two ZnO_4 tetrahedra and two methylendiphosphonate groups.[6c] Other examples are a vanadio-methylendiphosphonate showing a 3D structure with 14-membered windows[7] and the $Co_2(O_3P-CH_2-PO_3)\cdot H_2O$ with "rectangular" channels.[8]

On the other hand, Dines et al.[5a] were the first to introduce the use of phosphorous acid as a spacer between the inorganic $-PO_3Zr$ layers cross-linking with a rigid aryl group: 4,4′-biphenylylenbis(phosphonic) acid, $[H_2O_3P-C_{12}H_8-PO_3H_2]$. So, for the fully pillared state the biphenyl rings are spaced only 5.3 Å and no porosity is expected. However, by introducing spacer molecules, such as $-PO_3H$ groups, porosity should be expected because of the empty space due to the separation of the pillars. Although these materials were synthesized in aqueous media,[5a] Clearfield et al.[5f,9] have successfully prepared supermicroporous hybrids with Zr^{4+} and biphenyl and terphenylbisphosphonate pillars without using any spacer molecules by carrying out the reactions in DMSO or DMSO$-C_2H_5OH$ mixtures. These materials show low crystallinity but with a narrow distribution of pores in the 10−20 Å range and surface areas of ∼400 m^2/g for the biphenyl and ∼250−300 m^2/g for the terphenyl derivatives. Morevover, the sulfonation of the aromatic rings gave highly acid materials with potential applications as catalysts and proton conductors.[5g] Related compounds with divalent metals [$Cu(HO_3P-R-PO_3H)$,[10a] $Zn(HO_3P-R-PO_3H)$[10b] and $Zn_2(O_3P-R-PO_3)\cdot 2H_2O$[11] R═$C_6H_4$, $C_{12}H_8$] were obtained in aqueous medium and the crystal structures are known. These fully pillared bisphosphonates show very low surface areas as there is not available free space because the phenyl rings are closely packed. The replacement of some of the aryl rings by phosphate/phosphite groups led to compounds with slightly higher surface areas and with isotherms that suggest the presence of slit-shaped mesopores.[11]

In this paper, we first report the synthesis and structure of a new bisphosphonic acid, 4-(4′-phosphonophenoxy)-phenyl phosphonic acid, $[H_2O_3P-C_6H_4]_2-O$. This organic complex agent has been used to prepare a new family of organo−inorganic hybrid materials with transition metals (Mn, Fe, Co, Ni, Cu, and Zn). The syntheses, structural details, and thermal behaviors are reported.

Experimental Section

General Methods. Carbon and hydrogen contents were determined by elemental chemical analysis on a Perkin-Elmer 240 analyzer. Thermal analysis (TGA-DTA) data were recorded in air on a Setaram Labsys apparatus with a heating rate of 10 $Kmin^{-1}$ in air and using calcined Al_2O_3 as a reference standard. The water content was determined from the weight loss in the heating process at relatively low temperatures. Infrared spectra were recorded on a Shimadzu FTIR-8300 apparatus in the spectral range 4000−400 cm^{-1} by using dry KBr pellets containing approximately 2% of each sample. The absorption spectra were recorded on a Shimadzu UV-3100 spectrometer in the 200−1600 nm range, with $BaSO_4$ as reference standard. 4,4′-Biphenylylenebis(phosphonic acid), $H_2O_3PC_6H_4-C_6H_4PO_3H_2$, was synthesized as earlier reported.[5g]

$H_2O_3PC_6H_4-C_6H_4PO_3H_2$, $[(CH_3CH_2)_2O_3P-C_6H_4]_2-O$, and $[H_2O_3P-C_6H_4]_2-O$ were characterized by an NMR technique. NMR spectra in solutions were recorded on a Bruker WP-200 SY instrument, at 200 MHz for ^1H and 50.3 MHz for ^{13}C. Chemical shifts are given relative to the residual signal of solvents, δ_H 7.24 ppm and δ_C 77.0 ppm for deuteriochloroform, and δ_H 3.31 ppm and δ_C 49.0 ppm for methanol-d_4. Coupling constants are given in Hz.

Preparation of 4-[4′-(Diethoxyphosphoryl)phenoxy]phenylphosphonic Acid Diethyl Ester (I). All chemicals of reagent quality were used as purchased from Aldrich. The diethyl ester was prepared using a slight modification of the Michaelis−Arbuzov reaction[12] by following a process similar to that used in the synthesis of the 4,4′-biphenylylenebis(phosphonic acid).[5g] Bis-(4-bromophenyl)-ether (19.68 g, 60 mmol) and 150 mL of 1,3 diisopropylbenzene were added to a 500-mL three-neck flask fitted with a

(5) (a) Dines, M. D.; Di Giacomo, P. M.; Callahan, K. P.; Griffith, P. C.; Lane, R. H.; Cooksey, R. E. In *Chemically Modified Surfaces in Catalysis and Electrochemistry*; Miller, J. S., Ed.; ACS Symposium Series 192; American Chemical Society: Washington, DC, 1982; Chapter 12. (b) Clearfield, A. In *New Developments in Ion Exchange Materials*; Abe, M., Kataoka, T., Suzuki, T., Eds.; Kodansha Ltd.: Tokyo, 1991. (c) Alberti, G.; Costantino, U.; Marmottini, F.; Vivan, R.; Zapelli, P. *Angew. Chem., Int. Ed. Engl.* **1993**, *32*, 1557. (d) Alberti, G. In *Comprehensive Supramolecular Chemistry*; Alberty, G., Bein, T., Eds.; Pergamon: New York, 1996; vol. 7, p 151. (e) Cheetham, A. K.; Férey, G.; Loiseau, T. *Angew. Chem Int. Ed.* **1999**, *38*, 3268. (f) Clearfield, A.; Wang, Z. *J. Chem. Soc., Dalton Trans.* **2002**, 2937−2947. (g) Wang, Z.; Heising, J. M.; Clearfield, A. *J. Am. Chem. Soc.* **2003**, *125*, 10375−10383.

(6) See, for example: (a) Song, H.-H.; Zheng, L.-M.; Lin, C.-H.; Wang, X.-Q.; Gao, S. *Chem. Mater.* **1999**, *11*, 2388. (b) Stock, N,; Bein, T. *J. Solid State Chem.* **2002**, *167*, 330−336, and references therein. (c) Barthelet, K.; Merlier, C.; Riou-Cavellec, M.; Riou, D.; Férey, G. *J. Mater. Chem.* **2002**, *12*, 1132−1137, and references threrein. (d) Fu, R.-B.; Wu, X.-T.; Hu, S.-M.; Zhang, J.-J.; Fu, Z.-Y.; Du, W.-X. *Inorg. Chem. Commun.* **2003**, *6*, 827−829. (e) Bakhmutova, E. V.; Ouyang, X.; Medvedev, D. G.; Clearfield, A. *Inorg. Chem.* **2003**, *42*, 7046−7051. (f) Yin, P.; Peng, Y.; Zheng, L.; Gao, S.; Xin, X.-Q. *Eur. J. Inorg. Chem.* **2003**, 726−730. (g) Stock, N.; Guillou, N.; Bein, T.; Férey, G. *Solid State Sci.* **2003**, *5*, 629−634.

(7) Riou, D.; Baltazar, P.; Férey, G. *Solid State Sci.* **2000**, *2*, 127−134.

(8) Lohse, D. L.; Sevov, S. C. *Angew. Chem., Int. Ed. Engl.* **1997**, *36* (15), 1619−1621.

(9) Clearfield A. *Chem. Mater.* **1998**, *10*, 2801−2810.

(10) (a) Poojary, D. M.; Zhang, B.; Bellinghausen, P.; Clearfield, A. *Inorg. Chem.* **1996**, *35*, 4942−4949. (b) Poojary, D. M.; Zhang, B.; Bellinghausen, P.; Clearfield, A. *Inorg. Chem.* **1996**, *35*, 5254−5263.

(11) Zhang, B.; Poojary, D. M.; Clearfield, A. *Inorg. Chem.* **1998**, *37*, 1844−1852.

(12) Harvey, R. G.; Desombre, E. R. *Top. Phosphorus Chem.* **1964**, *1*, 57.

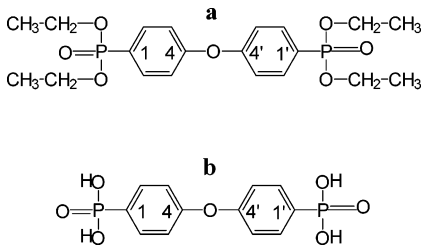

Figure 1. Schemes for 4-[4′-(diethoxyphosphoryl)phenoxy]phenyl phosphonic acid diethyl ester, **I**, and 4-(4′-phosphonophenoxy)phenyl phosphonic acid, **II**.

reflux condenser, N_2 inlet, and an addition funnel. The flask was fitted into a regulated heating mantle with magnetic stirring. The solution was heated to 70−80 °C after which 0.75 g of anhydrous $NiCl_2$ was added as catalyst. Immediately, the temperature was increased up to 180 °C. The flask was purged with N_2, and under a gentle stream of this gas, 30 mL (180 mmol) of triethyl phosphite was added over a 5-h period to minimize catalyst poisoning. This mixture was then heated at this temperature for 24 h followed by the addition of 0.69 g of fresh $NiCl_2$ to the solution and 30 mL of triethyl phosphite. This mixture was again heated for 24 h and allowed to cool overnight. The resulting dark black solution was vacuum distilled to remove the solvent and unreacted triethyl phosphite. The resulting dark liquid was kept at room temperature for several days until a sticky tar-like substance was formed. The ester was extracted with 500 mL of 40−60 °C petroleum ether in a Soxhlet extractor. After 10 days of extraction, the pet-ether was removed by rotary evaporation leaving an oily liquid. Mass spectroscopy of the ester showed a unique peak which agrees with the molecular weight calculated for $[Et_2O_3P-C_6H_4]_2-O$. The assignations of ^1H and ^{13}C NMR for **I** in $CDCl_3$ (Figure 1) are as follows. δ_H ($CDCl_3$) 7.81 (q, 4H, $J_{H,H} = 8.3$, $^3J_{H,P} = 15.8$, *ortho*-H), 7.12 (q, 4H, $J_{H,H} = 8.8$, $^4J_{H,P} = 3.6$, *meta*-H), 4.03 (m, 8H, C*H*$_2$), 1.29 (t, 12H, $J_{H,H} = 7.1$, C*H*$_3$). δ_C ($CDCl_3$) 159.4 (d, $^4J_{C,P} = 3.4$, C-4, C-4′), 133.8 (d, $^2J_{C,P} = 11.5$, C-2, C-6, C-2′, C-6′), 123.4 (d, $^1J_{C,P} = 192.8$, C-1, C-1′), 118.7 (d, $^3J_{C,P} = 11.5$, C-3, C-5, C-3′, C-5′), 61.9 (d, $^2J_{C,P} = 5.2$, *C*H$_2$), 16.2 (d, $^3J_{C,P} = 6.2$, *C*H$_3$).

Preparation of 4-(4′-Phosphonophenoxy)phenyl Phosphonic Acid (II). I was dissolved in 375 mL of ethanol and heated to 80 °C while stirring in a 500-mL three- neck flask. Concentrated HCl (150 mL) was added dropwise over a 3-h period by using an addition funnel. Then the transparent solution was heated. After the first day of hydrolysis, a white solid appeared. The process of hydrolysis was continued for 5 days more until no additional solid was observed. The solution was cooled and concentrated through rotary evaporation. The white solid was washed with large volumes of water and dried at 60 °C. The final white powder $[H_2O_3P-C_6H_4]_2-O$, 6.81 g, was obtained with a 57.2% yield based on $[BrC_6H_4]_2-O$.

Single crystals of **II** were obtained by dissolution of a small amount of the powder in the minimum amount of methanol and subsequent addition of ethanol to allow a slow crystallization. The methanol/ethanol molar ratio was 1:1. The assignations of ^1H and ^{13}C NMR for **II** in CD_3OD (Figure 1) are as follows. δ_H (CD_3OD) 7.82 (q, $J_{H,H} = 8.8$, $^3J_{H,P} = 13.1$, *ortho*-H), 7.13 (q, $J_{H,H} = 8.8$, $^4J_{H,P} = 3.2$, *meta*-H). δ_C (CD_3OD) 160.8 (d, $^4J_{C,P} = 3.5$, C-4, C-4′), 134.4 (d, $^2J_{C,P} = 11.4$, C-2, C-6, C-2′, C-6′), 128.5 (d, $^1J_{C,P} = 190.4$, C-1, C-1′), 119.9 (d, $^3J_{C,P} = 15.9$, C-3, C-5, C-3′, C-5′). Analytical data: experimental, C, 43.80%; H, 3.64%; calculated, C, 43.64%; H, 3.64%. The melting point of **II** is 271 °C.

Syntheses of M^{n+} 4-(4′-Phosphonophenoxy)phenyl Phosphonates. All compounds described below were prepared by adding the appropriate metallic salt, dissolved in water, to an aqueous suspension of **II**. The metal/acid molar ratio was always 2.1:1. The mixtures were heated in a 100-mL Teflon-lined autoclave for several days. Every product was filtered off, washed with water and acetone, and dried at 60 °C. The details for each synthesis as well as the elemental analyses are given in Table 1. The selected synthetic procedures shown in that table were those that gave single phase materials and/or higher yields.

Preparations of $Mn_2(O_3PC_6H_4OC_6H_4PO_3)\cdot 1.5H_2O$ (III) and $Mn_5(OH)_2(O_3PC_6H_4OC_6H_4PO_3)_2\cdot H_2O$ (IV). $Mn(CH_3COO)_2\cdot 4H_2O$ (Panreac, >99%, 0.515 g (2.1 mmol)) was dissolved in 20 mL of water and added to a 20 mL suspension of 0.33 g (1 mmol) of **II** under stirring. After 3 days of reaction under autogenous pressure at 200 °C, a very pale pink powder, **III**, was obtained. **IV** was prepared under the same conditions but the initial pH was increased up to 5.6 by adding 10 wt % aqueous solution of NaOH.

Preparation of $Fe(HO_3PC_6H_4OC_6H_4PO_3)\cdot 0.5H_2O$ (V). The hydrothermal experiments designed to prepare Fe^{2+} bisphopshonates gave a mixture of at least two phases: a thin dark green film at the bottom and a bright yellowish green powder (**V**) suspended. **V** was synthesized as a single phase by refluxing 0.584 g (2.1 mmol) of $FeSO_4\cdot 7H_2O$ (Prolabo, >99.5%) dissolved in 20 mL of water and a suspension of 0.33 g (1 mmol) of **II** in 20 mL of water. Although the starting source was an iron(II) salt, the obtained bisphosphonate contained trivalent iron.

Preparation of $Co_2(O_3PC_6H_4OC_6H_4PO_3)\cdot 2H_2O$ (VI). This compound was obtained as a purple powder from 0.534 g (2.1 mmol) of $Co(CH_3COO)_2\cdot 4H_2O$ (Panreac, >99%) and 0.33 (1 mmol) of acid in 22 mL of water.

Preparations of $Ni_2(O_3PC_6H_4OC_6H_4PO_3)\cdot 3H_2O$ (VII) and $Ni_2(O_3PC_6H_4OC_6H_4PO_3)\cdot 2H_2O$ (VIII). Several different syntheses led to the same stoichiometry but with different water contents. $Ni(CH_3COO)_2\cdot 4H_2O$ (Fluka, >99%, 0.543 g (2.18 mmol)) was mixed with a suspension of 0.34 g (1.03 mmol) of **II**. A first experiment was carried out for 5 days at 150 °C giving **VII**. A second preparation was carried out at 200 °C for 5 days giving **VIII**. If the initial pH was increased up to 5.5, by adding dropwise 25 wt % water solution of $[(CH_3)_4N]OH$, **VIII** was again formed but with higher yield. When the Ni^{2+} source was $NiSO_4\cdot 6H_2O$, pH 1.8, **VIII** was also obtained but with very low crystallinity and yield, 11%.

Preparation of $Cu_2(O_3PC_6H_4OC_6H_4PO_3)$ (IX). This compound was hydrothermally prepared from a mixture of 0.4234 g (2.1 mmol) of $Cu(CH_3COO)_2\ H_2O$ and 0.33 g (1 mmol) of **II** in 40 mL of water.

Preparations of $Zn_2(O_3PC_6H_4OC_6H_4PO_3)$ (X) and $Zn(HO_3PC_6H_4OC_6H_4PO_3H)$ (XI). Two zinc bisphosphonates were prepared with different starting compounds. $Zn(CH_3COO)_2\cdot 2H_2O$ (Panreac, >99.5%, 0.463 g (2.1 mmol)) and 0.33 g (1 mmol) of **II** were mixed in 40 mL of water and heated at 200 °C giving **X**. However, when 0.3769 g (2.1 mmol) of $ZnSO_4\cdot H_2O$ (Panreac, >99%) was used instead of the zinc acetate, the lower initial pH, see Table 1, yielded **XI**.

Crystallography and X-ray Data Collection for II. Single-crystal data were collected on a Bruker SMART 1000 CCD diffractometer equipped with monochromated Cu Kα radiation. Data collection and reduction were performed with Bruker CCD SMART 5.4 and SAINT+ 6.0 software.[13] Crystallographic comput-

(13) SMART version 5.0 and SAINT+ version 6.01 area detector instrument control, data acquisition and area detector data integration software; Bruker AXS, Inc. Madison, WI.

Table 1. Synthetic Conditions and Chemical Analyses for Divalent Transition Metal Bisphosphonates

compound	pH_i/pH_f	T (°C)/ t (days)	yield	chemical analysis: % found (% calcd) TGA: total Δm (%) = % found (% calcd) $\%H_2O$: % found (% calcd)
$Mn_2(O_3PC_6H_4OC_6H_4PO_3)\cdot 1.5H_2O$ (**III**)	4.7/3.3	200/3	93.5%	%C = 31.53 (31.11); %H = 2.38 (3.21) TGA: total Δm (%) = 36.0% (38.7) $\%H_2O$: 6.1% (5.8)
$Mn_5(OH)_2(O_3PC_6H_4OC_6H_4PO_3)_2\cdot H_2O$ (**IV**)	5.6/4.7	200/3	84.7%	%C = 29.43 (30.50); %H = 2.04 (2.99) TGA: total Δm (%) = 32.0% (32.9) $\%H_2O$: 5.0% (5.3)
$Fe(HO_3PC_6H_4OC_6H_4PO_3)\cdot 0.5H_2O$ (**V**)	1.9/1.6	Reflux/1	91.1%	%C = 36.72 (36.74); %H = 3.00 (2.55 TGA: total Δm (%) = 40.0% (43.6) $\%H_2O$: % 2.8 (2.3)
$Co_2(O_3PC_6H_4OC_6H_4PO_3)\cdot 2H_2O$ (**VI**)	4.5/4.0	200/5	90.4%	%C = 30.22 (30.01); %H = 2.78 (2.50) TGA: total Δm (%) = 40.2% (39.2) $\%H_2O$: 7.6% (7.5)
$Ni_2(O_3PC_6H_4OC_6H_4PO_3)\cdot 3H_2O$ (**VII**)	4.5/3.9	150/5	75.5%	%C = 29.85 (28.95); %H = 3.05 (2.81) TGA: total Δm (%) = 42.2% (41.4) $\%H_2O$: 11.3% (10.9)
$Ni_2(O_3PC_6H_4OC_6H_4PO_3)\cdot 2H_2O$ (**VIII**)	5.5/5.1	200/5	93.1%	%C = 29.39 (30.04); %H = 2.84 (2.5) TGA: total Δm (%) = 40.5% (39.2) $\%H_2O$: 8.4% (7.5)
$Cu_2(O_3PC_6H_4OC_6H_4PO_3)$ (**IX**)	4.8/4.0	200/3	88.7%	%C = 31.18 (31.78); %H = 1.69 (1.76) TGA: total Δm (%) = 32.5% (33.5)
$Zn_2(O_3PC_6H_4OC_6H_4PO_3)$ (**X**)	5.1/3.7	200/3	91.2%	%C = 32.00 (31.52); %H = 1.45 (1.75) TGA: total Δm (%) = 34.6% (33.3)
$Zn(HO_3PC_6H_4OC_6H_4PO_3H)$ (**XI**)	1−2/1.7	200/5	75.3%	%C = 35.97 (36.61); %H = 2.28 (2.54) TGA: total Δm (%) = 42.1% (43.2)

Table 2. Some Crystallographic Data for $[H_2O_3P-C_6H_4]_2-O$, **II** (single crystal); and $Cu_2(O_3PC_6H_4OC_6H_4PO_3)$, **IX**, and $Zn(HO_3PC_6H_4OC_6H_4PO_3H)$, **XI** (polycrystalline)

	II	**IX**	**XI**
empirical formula	$C_{12}H_{12}O_7P_2$	$Cu_2C_{12}H_8O_7P_2$	$ZnC_{12}H_{10}O_7P_2$
formula mass/g·mol^{-1}	330.16	453.16	393.43
dimensions/mm	0.05 × 0.04 × 0.01	powder	powder
temp/K	110(2)	∼300	∼300
wavelength/Å	1.542	1.542	1.542
space group	*Pbcn*	*Pbcn*	$P112_1$
a/Å	7.822(3)	8.1012(5)	9.4991(9)
b/Å	5.821(2)	5.3109(3)	5.0445(5)
c/Å	28.982(9)	29.260(1)	29.131(2)
γ/°			91.945(7)
V/Å^3	1319.7(7)	1258.9(2)	1395.1(3)
$V_{at-non-H}$/Å^3/at	15.71	13.65	15.93
Z	4	4	4
D_c/g·cm^{-3}	1.662	2.349	1.826
μ/mm^{-1}	3.18	6.47	4.60
F(000)	680	896	792
theta range for data collection (°)	3.05−58.97	$16 < 2\theta < 74.1$	$14 < 2\theta < 79.8$
index ranges	$8 \le h \le 5$, $-6 \le k \le 6$, $-32 \le l \le 25$		
reflns collected	4888		
independent reflns	896 [R(int) = 0.1147]	836	1783
refinement method	Full-matrix least-squares on F^2	Rietveld	Rietveld
data/restraints/params	896/0/96	836/31/70	1783/115/175
GOF on F^2, χ,	1.007	3.11	23.6
R indices [$I > 2\sigma(I)$]	R1 = 0.0614, wR2 = 0.1036	$R_F^2 = 0.064$	$R_F^2 = 0.102$
R indices [all data]	R1 = 0.1630, wR2 = 0.1306	$R_P = 0.024$, $R_{WP} = 0.030$	$R_P = 0.084$, $R_{WP} = 0.106$
largest diff. peak and hole	0.341 and −0.340 e·Å^{-3}		

ing was performed using the SHELXTL 5.10 package.[14] A small colorless platelet microcrystal of dimensions 0.05 × 0.04 × 0.01 mm^3 was used. The data collection details and some crystallographic information are given in Table 2.

Crystallography and X-ray Powder Data Collection for III−XI. X-ray powder diffraction patterns for the metal bisphosphonates were collected at room temperature on a Siemens D-5000 powder diffractometer using graphite-monochromated Cu Kα radiation. Higher statistics powder diffraction data were recorded for compounds **IX** and **XI** between 12 and 80° in 2θ with a step size of 0.02° and a counting time of 14 s per step. To minimize the preferred orientation effect, the powder patterns were collected in a sample disordered in the tubular aerosol suspension chamber (TASC) as previously reported.[15] Further details of the powder data collection and analysis are given in Table 2. The powder thermodiffractometric study for **VI** was carried out with the same diffractometer but in a second goniometer permanently equipped with an HTK 10 heating chamber. The thermodiffractometric pattern was scanned over the angular range 3−35° (2θ) and counting 1 s per step. The sample was held at each temperature for 10 min before recording any pattern to ensure that any transformations that may take place were allowed time to complete.

(14) Sheldrick, G. M. SHEXTL Crystallographic Software Package, Version 5.1; Bruker-AXS, Madison, WI, 1998.
(15) Cabeza, A.; Losilla, E. R.; Martínez-Tapia, H. S.; Bruque, S.; Aranda, M. A. G. *Adv. X-ray Anal.* **2000**, *42*, 228−237.

Results and discussion

Thermal Study. The thermal behaviors of the nine phosphonates are quite similar. In the Supporting Information, Figure S1, are shown, as archetypes, the TGA curves for compounds **VI**, **X**, and **XI**. The TG curve for **VI**, Figure S1a, is representative for compounds **III**−**VIII** as all contain hydration water molecules. This is evident as a weight loss at temperatures ranging between 140 and 250 °C. These losses are associated with endotherms. The combustion of the organic parts are observed above 400 °C, which are associated with exotherms. **VII**, which has three hydration water molecules, gave two weight losses prior to the combustion. One step is observed above 90 °C due to the release of one water molecule and a second loss above 250 °C corresponding to the remaining two water molecules. The TG curve for **X**, Figure S1b, is representative of anhydrous bisphosphonates (**IX** and **X**). There is only a weight loss starting at about 500 °C due to the combustion of the organic moieties. The TG curve for **XI**, Figure S1c, is representative of hydrogenbisphosphonates (**V** and **XI**). Prior to the organic combustion, a small loss, associated with an endotherm, is observed, and this is due to the condensation of the acid phosphonic groups (−POH) with the subsequent release of water.

The thermal decomposition products at 900 °C were identified through their X-ray powder patterns. Bisphosphonates **III** and **VI**−**X** gave the corresponding metal pyrophosphates, $M^{II}_2P_2O_7$, as the only crystalline compound. This result supports the 1:1 M/P ratio in the proposed formulas. The thermal residue for **IV**, a hydroxy bisphosphonate, was a mixture of $Mn_2P_2O_7$ and $Mn_3(PO_4)_2$, which agrees with the chemical formula having higher than 1.0 Mn/P molar ratio. Hydrogen bisphosphonates **V** and **XI**, with metal/P molar ratios of 0.5, gave poor crystalline compounds that could not be identified.

Infrared Spectroscopy Study. The IR spectra for the diphosphonic acids $H_2O_3PC_6H_4-C_6H_4PO_3H_2$ and $H_2O_3PC_6H_4OC_6H_4PO_3H_2$ (**II**) are shown in Figure 2a and b, respectively. Two very broad bands centered at 2850 and 2350 cm^{-1} denote the presence of the acid groups, PO−H, which interact strongly by H-bonds in both compounds. The first band is due to the PO−H stretching vibrations and the second band is usually assigned as a combination band of the P−O stretching vibrations, in agreement with IR data already reported.[16] The small sharp absorptions corresponding to the C_{ar}−H stretching vibrations are present at 3090 and 3070 cm^{-1}. The strong sharp absorptions at 1589, 1500, and 1404 cm^{-1} for **II**, see Figure 2b, are due to the $C_{ar}-C_{ar}$ stretching vibrations. The sharp band centered at 1260 cm^{-1} for **II** can be assigned to C_{ar}−O as it is absent in the IR spectrum of the 4,4′-biphenylylenebis (phosphonic acid), Figure 2a. In the 1200 and 1000 cm^{-1} range, a set of bands due to P−O stretching vibrations are located. Below 1000 cm^{-1}, many absorptions bands, characteristic of these phosphonic acids, are observed.

(16) Holmes, R. R.; Day, R. O.; Yoshida, Y.; Holmes, J. M. *J. Am. Chem. Soc.* **1992**, *114*, 1771.

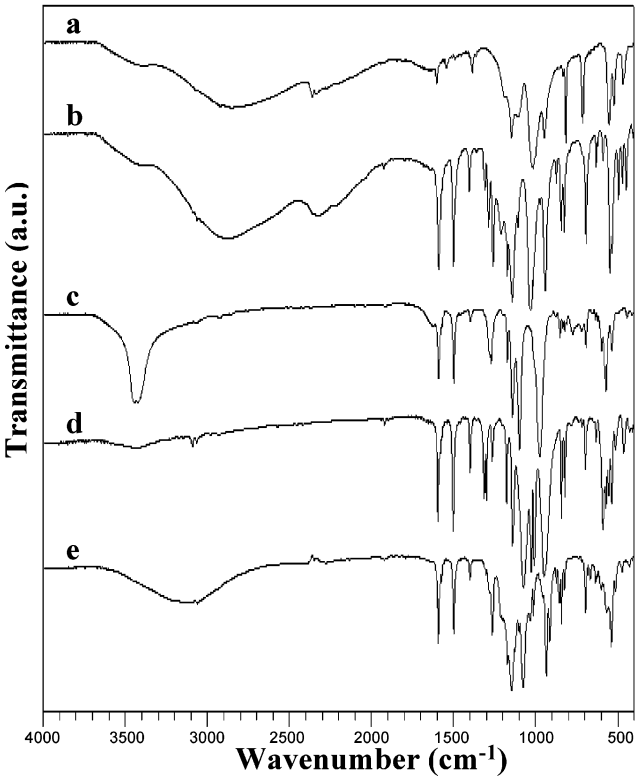

Figure 2. FTIR spectra for (a) $H_2O_3PC_6H_4-C_6H_4PO_3H_2$; (b) $H_2O_3PC_6H_4-OC_6H_4PO_3H_2$, **II**; (c) $Ni_2(O_3PC_6H_4OC_6H_4PO_3)\cdot 2H_2O$, **VIII**; (d) $Cu_2(O_3-PC_6H_4OC_6H_4PO_3)$, **IX**; and (e) $Zn(HO_3PC_6H_4OC_6H_4PO_3H)$, **XI**.

The IR spectra of the metal(II) bisphosphonates change, when compared to that of the pristine diphosphonic acid, due to the formation of the corresponding salt. Three representative infrared spectra have been selected and they are also displayed in Figure 2. Figure 2c shows the IR spectrum for **VIII** which is representative of the hydrated metal bisphosphonates **III**−**VIII**. It shows the O−H stretching vibrations of the water molecules centered close to 3400 cm^{-1} and the disappearance of the PO−H stretching vibrations. The H−O−H bending vibration of the water molecules in **VIII** is observed as a shoulder near 1620 cm^{-1}. Figure 2d shows the IR spectrum for **IX** which is representative of the anhydrous metal bisphosphonates, **IX**−**X**. O−H stretching vibrations are not detected, in agreement with the chemical formula. The bands are those typical of the organic group. Finally, Figure 2e shows the IR spectrum for **XI** which is representative of the anhydrous metal hydrogen bisphosphonates. The broad band centered at 3100 cm^{-1} is typical of the PO−H stretching vibrations but without strong interaction by H-bonds. There is no band in the H−O−H bending region, in agreement with the chemical formula.

Diffuse Reflectance Spectra. The absorption spectra of metal bisphosphonates are shown in Figure 3. The absorption spectrum for **IV** (Mn^{2+}-d^5), which has a pale pink color, is given in Figure 3a. The spectrum has two bands near 230 and 280 nm which are typical charge-transfer absorptions. These bands are present in all the synthesized bisphosphonates. The absence of any strong band in the visible range suggests that the oxygen environment around the manganese is octahedral. The absorption spectrum for **V** (Fe^{3+}-d^5), which

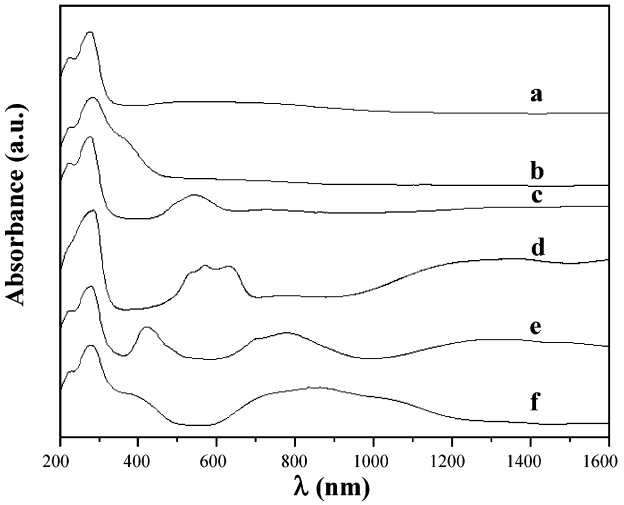

Figure 3. Diffuse reflectance spectra for (a) $Mn_2(O_3PC_6H_4OC_6H_4PO_3)\cdot 1.5H_2O$, **III**; (b) $Fe(HO_3PC_6H_4OC_6H_4PO_3)\cdot 0.5H_2O$, **V**; (c) $Co_2(O_3PC_6H_4OC_6H_4PO_3)\cdot 2H_2O$, **VI**; (d) $Co_2(O_3PC_6H_4OC_6H_4PO_3)$; (e) $Ni_2(O_3PC_6H_4OC_6H_4PO_3)\cdot 2H_2O$, **VIII**; and (f) $Cu_2(O_3PC_6H_4OC_6H_4PO_3)$, **IX**.

has a pale yellow color, is given in Figure 3b. Again, any d−d bands should be very weak and they are not observed. However, the greater oxidizing power of Fe(III) make the charge-transfer bands stronger, and a new charge-transfer band appears as a shoulder at 340 nm which justifies the color of this compound.

The absorption spectrum for **VI** (Co^{2+}-d^7), which has a purple color, is given in Figure 3c. The profile is typical of the CoO_6 octahedral groups with three bands. The main absorption is located close to 540 nm and it is assigned to the $^4T_{1g}(F) \rightarrow {}^4T_{1g}(P)$ transition. A second quite weak band is observed near 770 nm and it is due to the $^4T_{1g}(F) \rightarrow {}^4A_{2g}$ transition. The third band is close to 1320 nm and assigned to the $^4T_{1g}(F) \rightarrow {}^4T_{2g}$ transition.[17] After dehydration at 160 °C, purple **VI** transforms to blue $Co_2(O_3PC_6H_4OC_6H_4PO_3)$ and its absorption spectrum is given in Figure 3d. This new profile is typical of CoO_4 tetrahedral groups which shows two complex bands. The first band is centered at 1350 nm and is due to the $^4A_2 \rightarrow {}^4T_1(F)$ transition. The second band, due to the $^4A_2 \rightarrow {}^4T_1(P)$ transition, is observed between 530 and 630 nm, and its complexity is originated by several spin forbidden quartet−doublet transitions.[17] This complex band is located at lower energy than that of the octahedral CoO_6 groups, as seen in Figure 3, and it directly shows the change in the oxygen's environment from octahedral to tetrahedral upon dehydration.

The absorption spectrum for **VIII** (Ni^{2+}-d^8), which has a yellow color, is given in Figure 3e. The observed five bands are those typical for a NiO_6 octahedral environment. Three spin allowed bands are located at ∼1250, 780, and 420 nm which are assigned to the $^3A_{2g}$ to $^3T_{2g}$, $^3T_{1g}(F)$, and $^3T_{1g}(P)$ transitions, respectively. Two spin forbidden bands, located at ∼700 and ∼490 nm, are assigned to the $^3A_{2g}$ to ^1E_g and $^1T_{2g}$ transitions, respectively. Finally, the absorption spectrum for **IX** (Cu^{2+}-d^9), which has a yellowish green color, is given in Figure 3f. A new broad charge transfer band is observed close to 380 nm. Three broad strongly overlapped absorption bands are observed at approximately 1000, 840, and 740 nm. These peaks are consistent with copper in a very distorted CuO_5 oxygens environment, with four short Cu−O bonds and one very long Cu−O bond, due to the Jahn−Teller effect. A likely assignment of these bands are the transitions from z^2 to $x^2 - y^2$ at 1000 nm, from *xz*, *yz* to $x^2 - y^2$ at 840 nm, and from *xy* to $x^2 - y^2$ at 740 nm.[17]

(17) Lever, A. B. P. *Inorganic Electronic Spectroscopy*, 2nd ed.; Elsevier Science: New York, 1984.

Table 3. Bond Lengths (Å) and Angles (°) for $[H_2O_3P-C_6H_4]_2-O$, **II**

P1−O2	1.497(5)	O2−P1−O3	112.7(3)
P1−O3	1.529(5)	O2−P1−O4	112.2(3)
P1−O4	1.539(5)	O3−P1−O4	108.2(3)
P1−C4	1.743(7)	O2−P1−C4	110.9(4)
		O3−P1−C4	107.0(3)
		O4−P1−C4	105.6(3)
O1−C1 × 2	1.375(7)	C1−O1−C1	122.9(8)
C1−C2	1.366(10)	C2−C1−O1	116.8(7)
C1−C6	1.395(10)	C2−C1−C6	120.5(8)
C2−C3	1.349(9)	O1−C1−C6	122.7(7)
C3−C4	1.405(10)	C3−C2−C1	119.1(8)
C4−C5	1.388(9)	C2−C3−C4	123.6(8)
C5−C6	1.372(9)	C5−C4−C3	115.4(7)
		C6−C5−C4	122.5(7)
		C5−C6−C1	118.8(8)

X-ray Diffraction Study. Crystal Structure of $[H_2O_3P-C_6H_4]_2$-O, II. Structure solution and refinement was performed with the SHELXTL package[14] in the space group *Pbcn* ($a = 7.822(3)$ Å, $b = 5.821(2)$ Å, $c = 28.982(9)$ Å, $V = 1319.7(7)$, $Z = 4$, and $V_{at-non-H} = 15.71$ Å^3/at). The positions of the non-hydrogen atoms were located by direct methods and refined by full-matrix least squares on F^2 against all reflections. All non-hydrogen atoms were refined anisotropically. Hydrogen atoms were positioned from geometric considerations, included in the refinement, but their positions were not refined. Atomic parameters are given as Supporting Information in Table S1. Bond distances and angles are given in Table 3.

The crystal structure of **II** is given in Figure 4 with some atoms labeled. The oxygen atom corresponding to the ether function, O1, is situated on a 2-fold axis, and therefore, the asymmetric part of the unit cell contains a unique phenyl ring, C1−C6, and one phosphonic acid, P1 and O2−O4, see Table S1. The framework is layered with the diphenyl rings pointing along the *c*-axis. The angle between the phenyl rings is 122.9(8)°, C1−O1−C1, typical of the ether functions. As expected, the tetrahedral phosphonic group, CPO_3H_2, has two long P−O bonds at 1.53(1) Å, corresponding to the protonated oxygens, a shorter P═O distance at 1.497(5) Å, and a long P−C bond at 1.743(7) Å, see Table 3. There are two types of H-bonds. The interlayer H-bond, which holds the layers together, is O4−H2···O2 with distances O4···O2 of 2.57 Å and O4−H2···O2 angle of 154.6°, see Figure 4 (large dashed lines). There is a second intralayer H-bond, O3−H1···O2 with distances O3···O2 of 2.51 Å and O3−H1···O2 angle of 154.4 °, see Figure 4 (small dashed lines). The central phosphonic molecules shown in Figure 4 are displaced by half of the *b*-axis value, so they are not interacting with the adjacent phenyl rings through Phi−Phi interactions. The knowledge of the structural details of **II** is

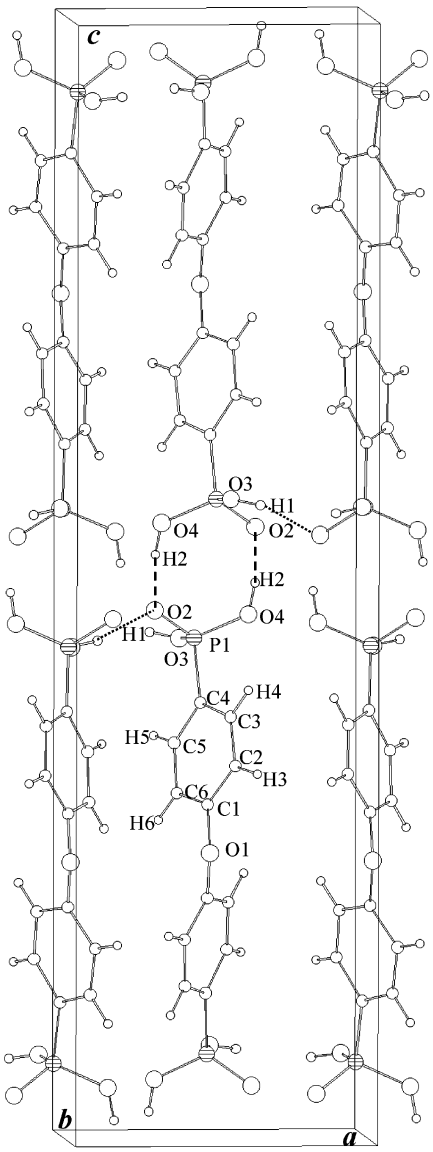

Figure 4. Ball and stick representation of the crystal structure of $(H_2O_3PC_6H_4)_2O$ with atoms labeled. The interlayer and intralayer hydrogen bond interactions are schematically highlighted as large and small dashed lines, respectively.

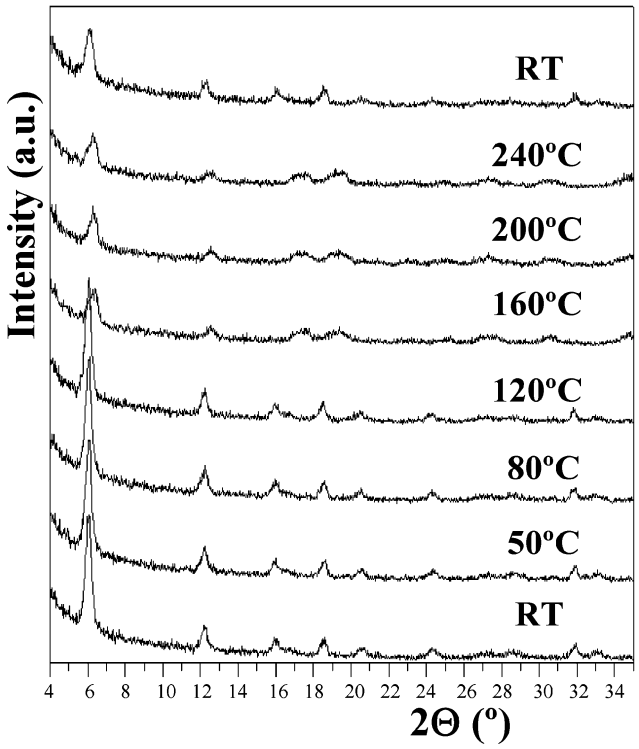

Figure 5. X-ray thermodiffraction for $Co_2(O_3PC_6H_4OC_6H_4PO_3)\cdot 2H_2O$.

Table 4. Selected Bond Lengths (Å) and Angles (°) for $Cu_2(O_3PC_4H_6OC_4H_6PO_3)$, **IX**

Cu−O1	1.92(2)	P−O1	1.546(3)	C1−C2	1.395(3)
	2.61(2)	P−O2	1.549(3)	C2−C3	1.410(3)
Cu−O2	1.93(6)	P−O3	1.539(3)	C3−C4	1.395(3)
	1.99(2)	P−C1	1.817(3)	C4−C5	1.412(3)
Cu−O3	1.92(2)			C5−C6	1.388(3)
				C6−C1	1.401(3)
C4−O4	1.339(3)	C4−O4−C4	117.2(6)		
O1−Cu−O2	96.6(12)	O2−Cu−O3	157.9(7)	O1−Cu−O3	94.29(3)
	163.2(7)		93.0(1)	O2−Cu−O2	81.81(3)
O1−P−O2	110.3(2)	O2−P−O3	110.8(2)	O2−P−C1	107.8(2)
O1−P−O3	111.1(2)	O1−P−C1	108.0(2)	O3−P−C1	108.6(2)
P−C1−C2	122.7(4)	C2−C3−C4	120.7(3)	C4−C5−C6	120.7(3)
P−C1−C6	115.9(3)	C3−C4−C5	117.9(3)	C1−C6−C5	119.6(4)
C2−C1−C6	117.5(4)	C3−C4−O4	125.5(6)		
C1−C2−C3	119.9(3)	C5−C4−O4	113.3(4)		

very important as the resulting hybrids do not have high crystallinities. So the bond distances and angles of **II** can be used as restraints in the structure determination procedures for the organo−inorganic compounds.

The first diffraction peak (002) for **II**, corresponding to the basal spacing, is observed at 14.49 Å. This value is larger than that of 4,4'-biphenylylenebis(phosphonic) acid, 13.06 Å. This increase is due to the introduction of the ether function between the phenyl rings. The powder pattern for 4,4'-biphenylylenebis(phosphonic) acid was auto-indexed using the TREOR90 program[18] in a monoclinic cell with $a = 7.149(5)$ Å, $b = 13.529(8)$ Å, $c = 13.118(7)$ Å, $\beta = 98.55(4)°$, $V = 1255(1)$ Å^3, $Z = 4$, $V_{at-non-H} = 15.68$ Å^3/at, $M_{20} = 8$,[19] and $F_{20} = 12$ (0.019, 108).[20] The volume per non-hydrogen atom is very similar to that of **II** but the cell edges are doubled along the *b*-axis and halved along the *c*-axis.

Structural Details for Hydrated Metal Bisphosphonates, III−VIII. Metal bisphosphonates have patterns with the first diffraction peak, corresponding to the basal spacing, ranging between 14.3 and 14.6 Å. This is very close to the interlayer spacing of the pristine solid **II**, 14.5 Å. The substitution of two protons for the metal(II) cations between adjacent layers makes a very minor modification of the interlayer distances, the metric of the cells change little, although the symmetry of the resulting compounds can be largely modified.

The X-ray powder diffraction patterns for **III−IV** and **VI−VIII** show broad peaks indicating low crystallinity and

(18) Werner, P. E.; Eriksson, L.; Westdahl, M. *J. Appl. Crystallogr.* **1985**, *18*, 367.

(19) Wolff, P. M. *J. Appl. Crystallogr.* **1968**, *1*, 108.
(20) Smith, G. S.; Snyder, R. L. *J. Appl. Crystallogr.* **1979**, *12*, 60.

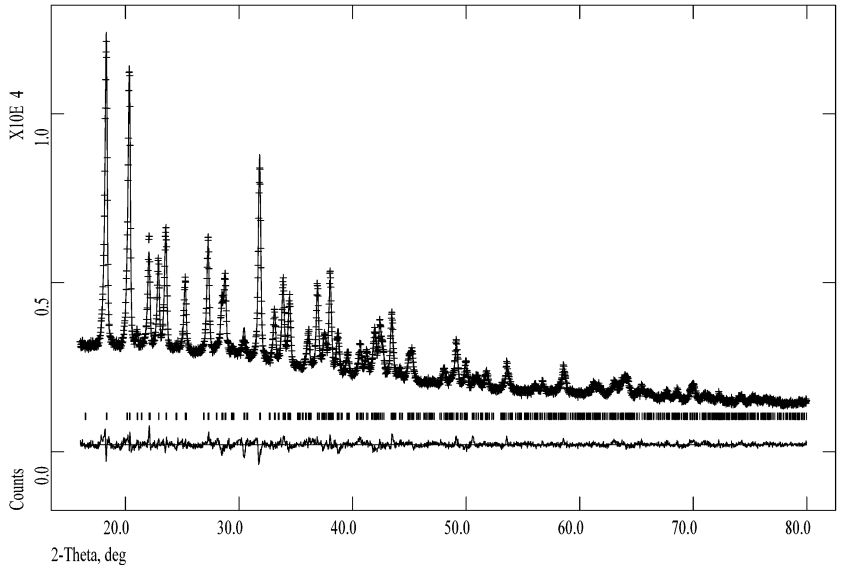

Figure 6. Final laboratory X-ray powder diffraction Rietveld plot for $Cu_2(O_3PC_6H_4OC_6H_4PO_3)$, **IX**.

their structures have not been solved. However, some insights can be obtained from the absorption spectroscopy studies. All hydrated materials have metals in oxygen octahedral environments with the water very strongly retained as determined in the thermal study. The releasing temperatures for the water molecules are higher than 150 °C which suggests that they may be directly bonded to the metals. The presence of these water molecules plus a larger disorder in the organic moieties may justify the lower crystallinity of these compounds when compared to the anhydrous ones (see below).

The X-ray laboratory powder pattern for **V** obtained hydrothermally, which has higher crystallinity than that obtained by refluxing, was auto-indexed using the TREOR90 program.[18] The resulting orthorhombic unit cell has a = 9.644(3) Å, b = 10.025(2) Å, c = 14.062(2) Å, V = 1359(1) Å^3, Z = 4, $V_{at-non-H}$ = 14.77 Å^3/at, M_{20} = 16,[19] and F_{20} = 31 (0.0163, 42).[20] The systematic absences indicated *Pmcm* as the possible highest symmetry space group. The cell edges are very related to those of metal bisphosphonates, see below, but doubling the *b*-axis and halving the *c*-axis. The crystal structure is under study by ab initio powder diffraction methodology.

VI has been studied in more detail as its color changes reversibly from purple, at room temperature, to deep blue above 160 °C. This is typical for a change in the oxygen environment from CoO_6 octahedral to CoO_4 tetrahedral. A thermodiffractometric study was undertaken to characterize this reversible evolution. Figure 5 shows the powder pattern of **VI** at several selected temperatures and finally at room-temperature again. A sharp modification is observed between 120 and 160 °C with a small contraction in the interlayer spacing. This topotactic change agrees with the water loss observed in Figure S1a. If this blue compound is exposed to the atmosphere at room temperature, it is rapidly hydrated and the purple solid with the original powder pattern is obtained. The crystallinity of $Co_2(O_3PC_6H_4OC_6H_4PO_3)$ obtained by dehydrating **VI** is poor, see Figure 5.

Crystal Structure of $Cu_2(O_3PC_6H_4OC_6H_4PO_3)$, IX. The X-ray laboratory powder pattern of **IX** was auto-indexed using the TREOR90 program[18] which gave an orthorhombic unit cell with a = 8.085(4) Å, b = 5.308(2) Å, c = 29.24(1) Å, V = 1255(1) Å^3, Z = 4, $V_{at-non-H}$ = 13.65 Å^3/at, M_{20} = 13,[19] and F_{20} = 21 (0.013, 74).[20] The systematic absences indicated *Pbcn* as the highest symmetry possible space group. The crystal structure was solved by an ab initio procedure from powder diffraction data. The pattern decomposition option of the GSAS package[21] was used to extract structure factors, using the Le Bail method,[22] from a limited region of the powder pattern, $16 < 2\Theta < 74.1°$ (836 reflections). Structure determination by direct methods was carried out using the programs Sir2002[23] by default setting. The best solution, after 200 trials and with an R residual value of 31.9%, gave the atomic positions for one copper atom, one phosphorus atom, three carbon atoms, and four oxygen atoms, three of which bond to the P atom and the fourth in a special position on the 2-fold axis, as for the ether oxygen in **II**. So, there were only three carbon atoms left to find for completing the phenyl ring. These three carbon atoms were positioned by using geometrical considerations in order to build the complete phenyl ring.

The structure was refined by the Rietveld method[24] with the GSAS suite of programs[21] using the overall parameters obtained in the last cycle of the Le Bail extraction. At this stage, the refinement of the model was carried out using soft constraints in the following bond distances [P−O, 1.53(1); P−C, 1.80(1); C−C, 1.40(2); and C(4)−O_{ether}, 1.35(2) Å] and nonbonding distances [O···O, 2.55(2); O···C(1),

(21) Larson, A. C.; von Dreele, R. B. *General Structure Analysis System (GSAS)*; Los Alamos National Lab. Rep. No. LA-UR-86-748; Los Alamos, NM, 1994.
(22) Le Bail, A.; Duroy, H.; Fourquet, J. L. *Mater. Res. Bull.* **1988**, *23*, 447.
(23) Burla, M. C.; Camall, M.; Carrozzini, B.; Cascarano, G. L.; Giacovazzo, C.; Polidori, G.; Spagna, R. Sir2002: a new Direct Methods program for automatic solution and refinement of crystal structures. *J. Appl. Crystallogr.* **2003**, *36*, 1103.
(24) Rietveld, H. M. *J. Appl. Crystallogr.* **1969**, *2*, 65.

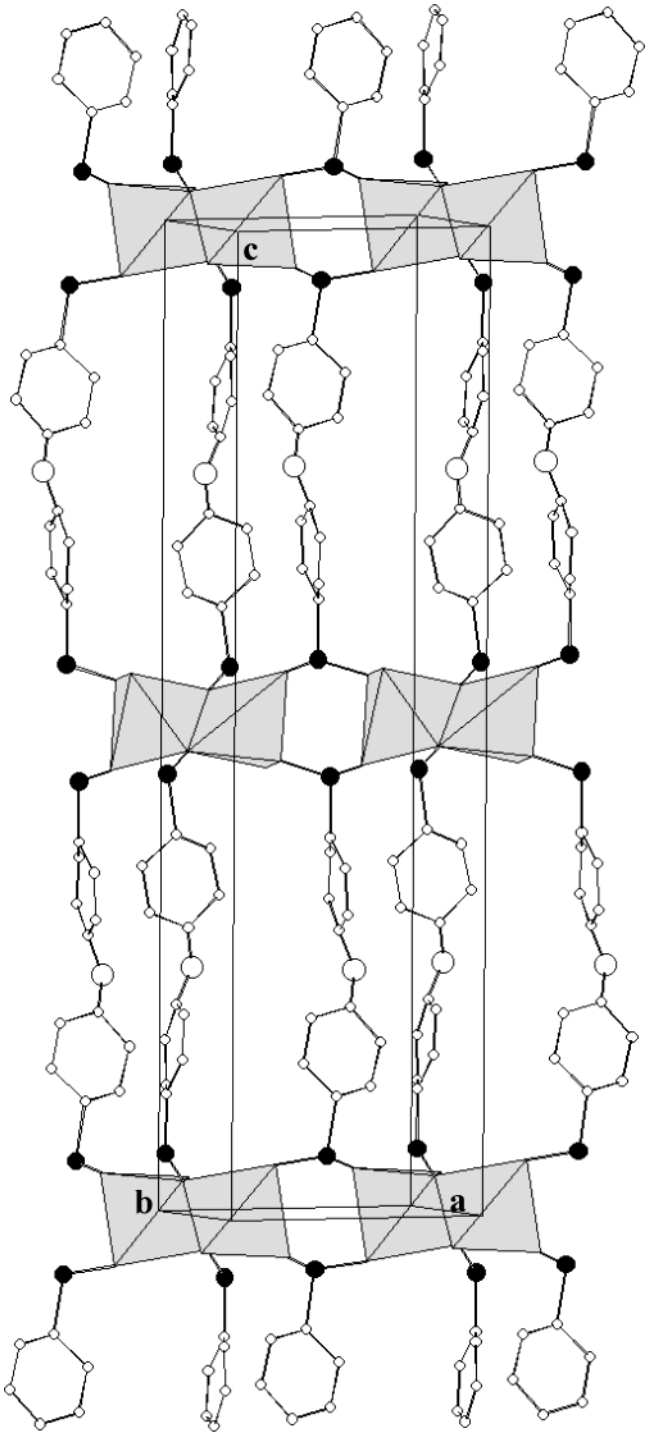

Figure 7. Ball and stick representation of the crystal structure of $Cu_2(O_3PC_6H_4OC_6H_4PO_3)$ with the oxygen polyhedra around the copper cations depicted.

2.73(1); C···C, 2.40(2); C···C, 2.78(2); and C(3/5)···O_{ether}, 2.40(2) Å] in order to keep a reasonable geometry for the tetrahedral O_3PC groups and a plane phenyl ring. Initially, the weight factor for the soft constraints was high, 200. The weight of the soft constraints was steadily reduced to the final value of 30. The preferred orientation along the [001] was refined using the March−Dollase[25] correction. The last refinement converged to $R_{wP} = 3.0\%$, $R_P = 2.4\%$, and $R_F = 4.2\%$. One isotropic thermal parameter was refined for

Table 5. Selected Bond Distances (Å) for $Zn(HO_3PC_4H_6OC_4H_6PO_3H)$, **XI**

Zn1−O2	2.05(2)	P1−O1	1.545(9)	P2−O4	1.547(9)
Zn1−O3	2.18(2)	P1−O2	1.540(9)	P2−O5	1.537(9)
Zn1−O6	1.95(2)	P1−O3	1.557(9)	P2−O6	1.551(9)
Zn1−O5B	1.94(3)	P1−C1	1.802(9)	P2−C7	1.829(9)
Zn1B−O5	2.06(3)	P1B−O1B	1.538(9)	P2B−O4B	1.545(9)
Zn1B−O2B	2.17(3)	P1B−O2B	1.547(9)	P2B−O5B	1.547(9)
Zn1B−O3B	2.10(2)	P1B−O3B	1.558(9)	P2B−O6B	1.545(9)
Zn1B−O6B	1.98(2)	P1B−C1B	1.81(1)	P2B−C7B	1.82(1)
		P1B−C6B	2.59(5)	P2B−C12B	2.47(4)
O7−C4	1.36(1)	O7B−C10	1.35(1)		
O7−C4B	1.36(1)	O7B−C10B	1.35(1)		

Cu atom, another for P atom, and a third one for the rest of the atoms (C and O). No attempts to locate the H atoms were carried out due to the limited quality of the powder diffraction data. Final positional and thermal parameters are given as Supporting Information in Table S2. Selected bond distances and angles are given in Table 4. The Rietveld refinement plot is shown in Figure 6.

The crystal structure of **IX** is displayed in Figure 7. The framework is layered with the inorganic layers built up by CuO_5 units. Four Cu−O short bond distances range between 1.92(2) and 1.99(2) Å, see Table 4, and there is a fifth very long distance to O(1) at 2.61(2) Å. It must be underlined that the two CuO_5 units share an edge giving isolated dimers in the inorganic layer. The biphenylylenebis(phosphonate)-ether organic groups act as pillaring agents along the *c*-axis and they are situated above and below the plane defined by the Cu cations. The C−O−C bond angle of the ether group is 117.2(6)° being close to the value found for **II**, 123°, given above. The layered structure of **IX** gave a basal spacing of 14.63 Å.

Crystal Structures of $Zn_2(O_3PC_6H_4OC_6H_4PO_3)$, X, and $Zn(HO_3PC_6H_4OC_6H_4PO_3H)$, XI. The X-ray powder diffraction pattern for **X** was auto-indexed using the TREOR90 program[18] in an orthorhombic cell with parameters a = 9.335(8) Å, b = 10.486(3) Å, c = 29.063(9) Å, V = 2855(1) Å^3, $Z = 8$, $V_{at-non-H} = 14.86$ Å^3/at, $M_{20} = 5$,[19] and $F_{20} = 11$ (0.021, 97).[20] This cell is very large since the *b*-axis is doubled when compared to those of the starting material, **II**, and the analogous copper hybrid, **IX**. All attempts to solve the crystal structure of **X** have been unsuccessful. However, the profile of its powder pattern is quite similar to that of **IX**. So, the framework of **X** must be very related to that of **IX**.

The X-ray powder pattern for **XI** was auto-indexed in a monoclinic unit cell using the TREOR90 program.[18] The parameters were a = 9.543(5) Å, b = 5.043(2) Å, c = 29.16(1) Å, $\gamma = 91.80(3)°$, $V = 1402(1)$ Å^3, $Z = 4$, $V_{at-non-H}$ = 15.93 Å^3/at, $M_{20} = 17$,[19] and $F_{20} = 43$ (0.011, 41).[20] The systematic absences were consistent with the space group $P112_1/m$. The obtained unit cell edges for **XI** were very close to that previously reported[10b] for the zinc biphenylylenebis(hydrogenphosphonate), $Zn(HO_3PC_{12}H_8PO_3H)$ [a = 9.510 Å, $b = 5.007$ Å, $c = 14.211$ Å, $\alpha = 92.80°$, $\beta = 99.73°$, γ = 92.03°, V = 665.5 Å^3, Z = 2, and space group $P\bar{1}$]. Therefore, this structure was used as a starting model for

(25) Dollase, W. A. *J. Appl. Crystallogr.* **1986**, *19*, 267.

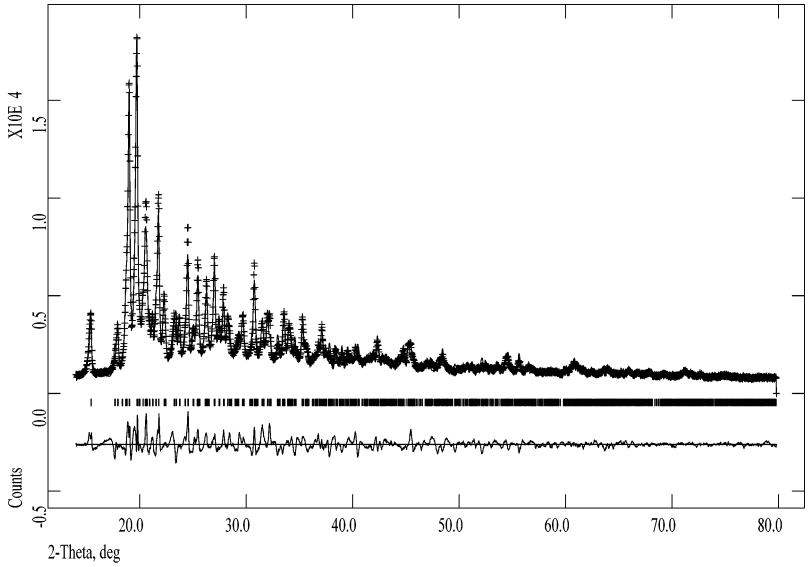

Figure 8. Final laboratory X-ray powder diffraction Rietveld plot for $Zn(HO_3PC_6H_4OC_6H_4PO_3H)$, **XI**.

the Rietveld refinement of $Zn(HO_3PC_6H_4OC_6H_4PO_3H)$ using the GSAS suite of programs[21]. Initially, the refinement was carried out in the space group $P112_1/m$ by including the two extra oxygen atoms in a special position (x, y, 0.25) corresponding to the ether function between the phenyl rings. The refinement was carried out using soft constraints for the bonding distances [Zn−O, 2.0(1); P−O, 1.53(1); P−C, 1.80(1); C−C, 1.40(2); and C(4)−O_{ether}, 1.35(2) Å] and nonbonding distances [O···O, 2.55(2); O···C(1), 2.73(1); C···C, 2.40(2); C···C, 2.78(2); and C(3/5)···O_{ether}, 2.40(2) Å] to keep a reasonable geometry for the tetrahedral O_3PC groups and a plane phenyl ring. The initial weight was 200 and was reduced in the successive cycles. At this point, the refinement did not converge. Hence, the refinement was carried out in the noncentrosymmetric space group $P112_1$. With this symmetry, there are 44 atoms in the asymmetric part of the unit cell: 2 Zn atoms, 2 ether oxygen atoms, and 4 different $HO_3P-C_6H_4$ units. Finally, the refinement converged to $R_{WP} = 10.6\%$, $R_P = 8.4\%$, and $R_F = 5.4\%$. The final weight of the soft constraints was 30 and the preferred orientation was refined using the March−Dollase[25] correction along the [001]. One isotropic thermal parameter was refined for all atoms. Final atomic positional parameters are given as Supporting Information in Table S3. The bond lengths are given in Table 5 and bond angles are provided as Supporting Information in Table S4. The Rietveld refinement plot is shown in Figure 8.

The crystal structure of **XI** is displayed in Figure 9 and it is very similar to that of zinc biphenylylenebis(hydrogenphosphonate)[10b] but with the ether function between the phenyl rings. The framework is layered with the inorganic layers built up by isolated ZnO_4 units. There are two crystallographically independent ZnO_4 tetrahedra with Zn−O bond distances ranging between 1.94(3) and 2.18(2) Å. The inorganic layer is formed by the linking of these tetrahedra through the phosphonate units along the b-axis. However, the inorganic layers are held together along the a-axis only by H-bonds of the phosphonic acid groups, see Figure 9, however, it must be noted that the hydrogens have not been located in this powder diffraction study. The biphenylylenebis(phosphonate)-ether organic groups act as pillaring

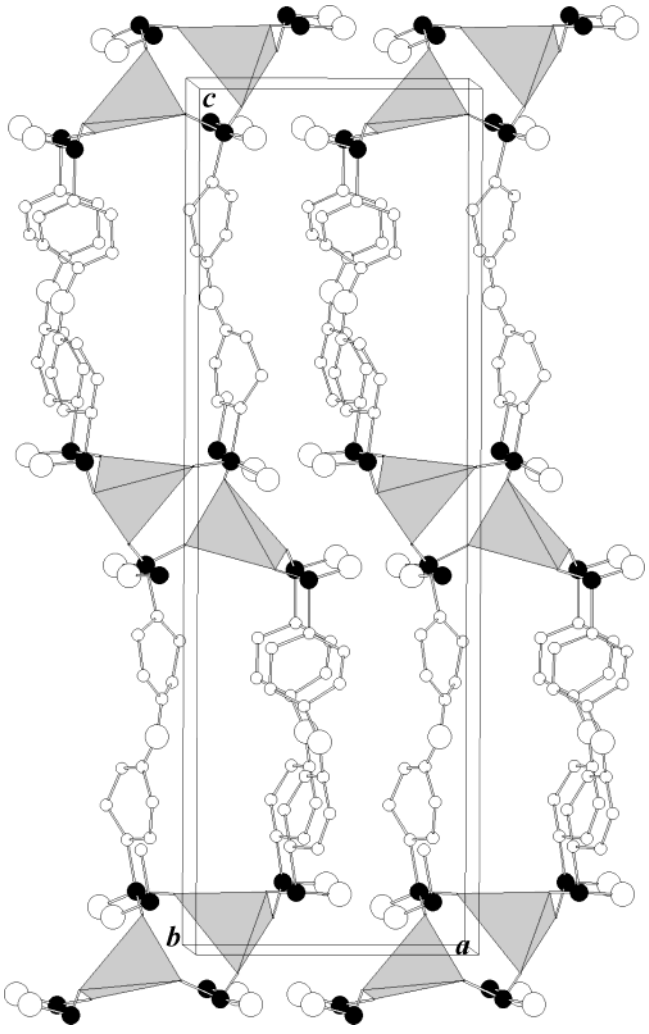

Figure 9. Ball and stick representation of the crystal structure of $Zn(HO_3PC_6H_4OC_6H_4PO_3H)$ with the ZnO_4 tetrahedral groups depicted.

agents along the *c*-axis. The layered structure of **XI** gave a basal spacing of 14.58 Å.

General Discussion

We have synthesized a new bisphosphonic acid, **II**, and its structure has been studied in detail. **II** has been used to prepare a new family of metal bisphosphonates. Although the metal/phosphonic acid molar ratio has been kept constant at 2.1/1, the use of acetate or sulfate as the source of the metallic ion may lead to compounds with different stoichiometries. This is a clear consequence of the acid nature of these starting salts that give quite different initial pH values for the syntheses. Thus, when the used salt is acetate, the initial pH is higher than 4 and the solids obtained have a formula $M_2(O_3PC_6H_4OC_6H_4PO_3)\cdot nH_2O$, **III** and **VI**−**X**. The use of a sulfate salt causes a decrease in the pH, approximately to 2, which favors the presence of protonated oxygen atoms in the phosphonate groups as was observed for **V** and **XI**. Furthermore, if the pH is artificially increased, hydroxy metal phosphonates can be obtained as was observed for **IV**. However, the pH is not the only key parameter as, for example, when a nickel(II) sulfate was used, the obtained compound was not protonated, although the pH was low. Hence, the metal oxygen environment is another key parameter. Finally, it must be pointed out that the starting metal source for **V** was Fe(II) sulfate, but **V** contains Fe(III) cations. The oxidation of Fe^{2+} to Fe^{3+} by the oxygen present in the reaction medium is likely due to two factors, the reducing character of Fe(II) plus the low solubility of the bisphosphonic acid in water that makes the reaction progress slowly with the O_2 dissolved in the refluxed water. Hydrothermal conditions do not allow full oxidation of Fe^{2+} to Fe^{3+} leading to a mixture of phases. However, the crystallinity of **V** obtained by refluxing is lower than that when it is hydrothermally obtained.

The oxygen environments around the metal cations in these hybrid materials may be octahedral or tetrahedral. The hydrated compounds, **III**−**VIII**, show features typical of MO_6 octahedra with water molecules directly bonded to the metals. These hybrids are less crystalline than the anhydrous counterparts. This may be due to the disorder imposed into the organic groups by the presence of the water molecules in the inorganic layers. On the other hand, the three anhydrous hybrids, **IX**−**XI**, have the metal in distorted MO_4−MO_5 polyhedra. These results are in full agreement with previously reported crystal structures for related materials. Hence, $Zn_2(O_3P(C_6H_4)_2PO_3)\cdot 2H_2O$ has a crystal structure with ZnO_6 octahedra in the inorganic layers[11] and anhydrous $Zn(HO_3P(C_6H_4)_2PO_3H)$[10b] and $Cu(HO_3P(C_6H_4)_2PO_3H)$[10a] hybrids have MO_4 polyhedra.

The three-dimensional crystal structures of these hybrid materials can be described as microcrystalline phases with an inorganic layer built up by the metal oxygen polyhedra which are pillared along the *c*-axis by the organic chelating group. In the present case, an ether function has been introduced between the phenyl rings of the phosphonic acid to increase the reactivity of these solids. The oxygen bonded to the aromatic rings acts as an electron donor and hence, it activates the ring for electrophilic aromatic substitutions (for example, sulfonation). In a next step, porosity may result by replacing part of the phosphonic groups by phosphate or phosphite. Finally, sulfonation can increase the acidity leading to acid porous catalysts.[5f,g] This work has been undertaken and results will be reported elsewhere.

Acknowledgment. Financial support from MCyT (Spain) through MAT2003-7483-C2-1 research grant and from R.A. Welch Foundation (United States) through A673 grant and NSF grant (United States) DMR-0332453 is gratefully acknowledged.

Supporting Information Available: X-ray crystallographic information in CIF format for compounds **II**, **IX**, and **XI**. Tables of refined atomic parameters for compounds **II**, **IX**, and **XI**; table of the selected bond angles for **XI**; and thermal analysis curves for **VI**, **X**, and **XI** (pdf). This material is available free of charge via the Internet at http://pubs.acs.org.

IC049453L